Franck-Condon factors perturbed by damped harmonic oscillators: Solvent enhanced X 1Ag ↔ A1B1u absorption and fluorescence spectra of perylene

Chen-Wen Wang, Ling Yang, Chaoyuan Zhu, Jian-Guo Yu, and Sheng-Hsien Lin

Citation: The Journal of Chemical Physics **141**, 084106 (2014); doi: 10.1063/1.4893529
View online: http://dx.doi.org/10.1063/1.4893529
View Table of Contents: http://scitation.aip.org/content/aip/journal/jcp/141/8?ver=pdfcov
Published by the AIP Publishing

Franck-Condon factors perturbed by damped harmonic oscillators: Solvent enhanced X $^1A_g \leftrightarrow A^1B_{1u}$ absorption and fluorescence spectra of perylene

Chen-Wen Wang,[1,a)] Ling Yang,[1,2,a)] Chaoyuan Zhu,[1,b)] Jian-Guo Yu,[3] and Sheng-Hsien Lin[1]

[1]*Institute of Molecular Science, Department of Applied Chemistry and Center for Interdisciplinary Molecular Science, National Chiao-Tung University, Hsinchu 30050, Taiwan*
[2]*Institute of Theoretical and Simulation Chemistry, Academy of Fundamental and Interdisciplinary Science, Harbin Institute of Technology, Harbin 150080, People's Republic of China*
[3]*Department of Chemistry, Beijing Normal University, Beijing 100875, People's Republic of China*

(Received 3 June 2014; accepted 8 August 2014; published online 25 August 2014)

Damped harmonic oscillators are utilized to calculate Franck-Condon factors within displaced harmonic oscillator approximation. This is practically done by scaling unperturbed Hessian matrix that represents local modes of force constants for molecule in gaseous phase, and then by diagonalizing perturbed Hessian matrix it results in direct modification of Huang–Rhys factors which represent normal modes of solute molecule perturbed by solvent environment. Scaling parameters are empirically introduced for simulating absorption and fluorescence spectra of an isolated solute molecule in solution. The present method is especially useful for simulating vibronic spectra of polycyclic aromatic hydrocarbon molecules in which hydrogen atom vibrations in solution can be scaled equally, namely the same scaling factor being applied to all hydrogen atoms in polycyclic aromatic hydrocarbons. The present method is demonstrated in simulating solvent enhanced X $^1A_g \leftrightarrow A^1B_{1u}$ absorption and fluorescence spectra of perylene (medium-sized polycyclic aromatic hydrocarbon) in benzene solution. It is found that one of six active normal modes v_{10} is actually responsible to the solvent enhancement of spectra observed in experiment. Simulations from all functionals (TD) B3LYP, (TD) B3LYP35, (TD) B3LYP50, and (TD) B3LYP100 draw the same conclusion. Hence, the present method is able to adequately reproduce experimental absorption and fluorescence spectra in both gas and solution phases. © *2014 AIP Publishing LLC*. [http://dx.doi.org/10.1063/1.4893529]

I. INTRODUCTION

The Franck-Condon factor plays a very important role for theoretical modeling and interpreting of experimental observations such as electronic spectra like VUV absorption and fluorescence, and also nonradiative processes like electron and energy transfer. Under Born-Oppenheimer approximation, Franck-Condon (FC) factor can be decomposed into a product of electronic factor and nuclear factor. The electronic factor is called as electronic transition dipole element for absorption and fluorescence spectroscopy and as nonadiabatic coupling matrix element (or vibronic coupling) for nonradiative processes. The nuclear factor described as vibrational overlap integral between two different electronic states is the same for both irradiative and nonradiative processes. With further harmonic oscillator approximation involving in normal mode coordinates, the number of methods and algorithms of multidimensional Franck–Condon factors for polyatomic species have been proposed and developed with or without including anharmonic correction.[1–17]

The theoretical treatment of solvent effects on irradiative and nonradiative processes is also divided into two parts. The electronic factor involves in modification of electronic transition dipole momentum and nonadiabatic coupling matrix under solvent environment. The nuclear factor involves with modification of multidimensional Franck–Condon factors due to equilibrium geometry change from gas phase to solution phase. The most popular theoretical approach for electronic factor of solute molecules in solution is conventionally represented by continuum solvation models, especially that the polarizable continuum model (PCM) combined with the time-dependent density functional theory (TDDFT) and this was developed to treat excited states for large polyatomic molecules.[18–20] Electronic ground- and excited-state equilibrium geometries, oscillator strength and excitation energy are calculated within TDDFT-PCM method for solvated molecular systems. Furthermore, the solvent effects on the absorption and fluorescence spectra have been well investigated within FC principle framework.[21–42] By introducing an average solvent interaction to all normal modes of molecular vibrations, inhomogeneous broadening approach in FC factor has been utilized to describe interaction between vibronic excited state of solute molecule and solvent.[15,16,37,38] By introducing time dependent approach as well as time-independent algorithm including Franck-Condon factors, Herzberg–Teller and Duschinsky effects, both high resolution of electronic spectra in gas phase and how these effects affect electronic spectra in solution have been investigated.[39–42] Detailed comparisons of those effects have been demonstrated

[a)]C.-W. Wang and L. Yang contributed equally to this work.
[b)]Author to whom correspondence should be addressed. Electronic mail: cyzhu@mail.nctu.edu.tw

for electronic spectra subject to environment change of solvents.[39]

The purpose of the present paper is to address that solute-molecule vibrations in solution are subjected to a damping force and to study how the damped harmonic oscillators affect electronic spectra of solute molecule. A displaced harmonic oscillator approximation is starting point, namely vibrational frequencies of solute molecule being the same for ground and excited electronic states. Furthermore, multidimensional FC factors can be decomposed into a product of many one-dimensional (1D) FC factors, and each 1D-FC factor is associated with one Huang–Rhys factor that determines the leading contribution of band shape and intensity of corresponding normal-mode vibronic spectrum.

The rest of this paper is organized as follows: Sec. II first introduces that damped diatomic oscillators in solution can be solved exactly in terms of one damping parameter. This damping parameter can be practically converted to scaled local force constant from undamped harmonic diatomic oscillators. Then, we extend the diatomic oscillators to the polyatomic oscillators by scaling the Hessian matrix from the corresponding isolated molecule. Each element of the Hessian matrix can be considered as diatomic-like local oscillators corresponding one damping parameter. All damping parameters are empirically determined from simulated electronic spectra in solution with comparison to experimental observation. The present algorithm is stimulated from inhomogeneous broadening that can be different for vibrational normal mode associated with ionic and neutral molecule in solution for reproducing absorption and fluorescence spectra of the green fluorescent protein chromophore.[43] Section III applies the present method to the perylene in benzene solution and shows that the present method is able to adequately reproduce experimental absorption and fluorescence spectra both in the gas phase and in solution. There are two reasons to choose the perylene as an example; one is that simulated absorption and fluorescence spectra showed very small Duschinsky and Herzberg−Teller effects in gas phase,[44] and the other is that there are quite large solvent enhanced electronic spectra from experiment observation.[45] We guess that strong interaction between solute and solvent results in direct modification of the Huang–Rhys factors and this is responsible for solvent enhanced electronic spectra. Polycyclic aromatic hydrocarbon molecules like the perylene have high symmetry in which each hydrogen atom is subjected to the same environment in solution, and thus scaled force constant to hydrogen atom can be considered as the same. This greatly simplifies empirical search of the damping parameters. We have carefully checked robustness in terms of change of the damping parameters by performing with (TD)-B3LYP, (TD)-B3LYP35, (TD)-B3LYP50, and HF-CIS *ab initio* quantum chemistry methods. Concluding remarks are mentioned in Sec. IV.

II. DAMPED HARMONIC OSCILLATOR METHOD

Suppose that diatomic harmonic oscillator AB is placed in solution subject to a damping force,

$$\mu_{AB}\ddot{R}_{AB} + k^0_{AB}R_{AB} = -\lambda\dot{R}_{AB}, \tag{1}$$

where damping parameter λ is positive, μ_{AB} and k^0_{AB} are reduced mass and unperturbed force constant respectively, and then unperturbed vibrational frequency $\omega^0_{AB} = \sqrt{k^0_{AB}/\mu_{AB}}$ is converted to perturbed vibrational frequency $\omega_{AB} = \sqrt{k_{AB}/\mu_{AB}}$ in which perturbed force constant is given by[46]

$$k_{AB} = k^0_{AB}\left(1 - \frac{\lambda^2}{4\mu_{AB}k^0_{AB}}\right) \equiv k^0_{AB}\frac{1}{\xi_{AB}}, \tag{2}$$

where ξ_{AB} can be considered as a scaling parameter converted from the damping parameter λ. We generalize above description to polyatomic system by transferring the mass-weighted unperturbed Hessian matrix to perturbed Hessian matrix,

$$H^0_{i\alpha,j\beta} = \frac{k^0_{i\alpha,j\beta}}{\sqrt{m_i m_j}} \rightarrow \frac{k^0_{i\alpha,j\beta}}{\sqrt{(m_i\xi_i)(m_j\xi_j)}} = \frac{k_{i\alpha,j\beta}}{\sqrt{m_i m_j}} = H_{i\alpha,j\beta}, \tag{3}$$

where m_i and m_j are atomic mass and α and β are Cartesian component (x, y, z) of the position of nucleus i and j. Unperturbed local force constant is converted to perturbed force constant by $k_{i\alpha,j\beta} = k^0_{i\alpha,j\beta}/\sqrt{\xi_i\xi_j}$. By diagonalizing perturbed Hessian matrix in Eq. (3), we obtain normal-mode frequencies and transformation matrix (that transfers the mass-weighted Cartesian coordinates to normal mode coordinates) corresponding to solute molecule under damped solvent environment. The dimensionless scaling parameter ξ_j in Eq. (3) is treated as an empirical parameter that reflects a local dynamic interaction of atom j of solute molecule with solvent molecule in the present study. In other words, the scaling parameters are empirically determined from simulated electronic spectra in solution with comparison to experimental observation. Physical meanings of the scaling parameters are obvious in which unperturbed local vibrational modes in gas phase are scaled to perturbed local vibrational modes in solution phase. After diagonalizing perturbed Hessian matrix in Eq. (3), we obtain both perturbed normal-mode harmonic vibrational frequencies and their corresponding perturbed normal-mode coordinates that represent an effective interaction between atoms of solute molecule and molecules of solvent. An alternative interpretation to damping (a solute friction or viscosity) can be that rather than scaling the force-constant matrix entries one views the phenomena in terms of scaling the masses of the atoms in the solute. The physical phenomena would be that in a full simulation including explicit solvent molecules there is a slight mixing of solvent motion with the atomic motions in the solute. In as sense the atoms in the solute drag along, partially, solvent molecules, resulting in increasing atom mass in the solute. Mathematically, both pictures result in a similar change of the model (and scale factors), however the interpretation is significantly different. In the latter picture, it seems clear that the high symmetry of perylene can lead to only few scaling parameters. In general this could be more complicated. In summary, the dimensionless scaling parameter ξ_j in Eq. (3) can be considered as either scaling force constant or scaling mass. It may be possible to simulate this empirical parameter by putting diatomic molecule in solution in the framework of QM/MM simulation. Diatomic molecule is treated quantum mechanically and

solution is treated from force field, and then perturbed force constant can be obtained to be compared with unperturbed one to extract the scaling parameter. This scaling parameter is mostly solvent depended and it can be defined for each solvent. This procedure is similar to the PCM model in which different dielectric constant is defined for different solvent to simulate electronic structure of solute.

Within displaced harmonic oscillator approximation, absorption and fluorescence coefficients can be analytically given by[15,16]

$$\alpha(\omega) \propto \omega \int_{-\infty}^{\infty} dt\, e^{it(\omega_{ba}-\omega)-\frac{D_{ba}^2 t^2}{4}-\gamma_{ba}|t|} \times \exp\left[-\sum_j S_j\left\{2\bar{\upsilon}_j + 1 - (\bar{\upsilon}_j + 1)e^{it\omega_j} - \bar{\upsilon}_j e^{-it\omega_j}\right\}\right] \tag{4}$$

and

$$I(\omega) \propto \omega^3 \int_{-\infty}^{\infty} dt\, e^{-it(|\omega_{ba}|-\omega)-\frac{D_{ba}^2 t^2}{4}-\gamma_{ba}|t|} \times \exp\left[-\sum_j S_j\left\{2\bar{\upsilon}_j + 1 - (\bar{\upsilon}_j + 1)e^{it\omega_j} - \bar{\upsilon}_j e^{-it\omega_j}\right\}\right], \tag{5}$$

where ω_{ab} represents electronically adiabatic excitation energy between electronic state b and a. Other quantities like $\bar{\upsilon}_j = (e^{\hbar\omega_j/k_B T} - 1)^{-1}$ is the average phonon distribution, γ_{ab} and D_{ab} represent the homogeneous and inhomogeneous broadenings, respectively, and ω_j and d_j are the jth normal-mode vibrational frequency and corresponding the displacement. The Huang-Rhys factor S_j (corresponding to the jth normal mode) can be calculated in both gaseous phase and solution phase by

$$S_j = \frac{1}{2\hbar}\omega_j d_j^2, \tag{6}$$

from the method proposed above. The present method indeed results in direct solvent modification of the leading contribution of electronic spectra in terms of the Huang-Rhys factors. Equations (4) and (5) can be utilized for both unperturbed and perturbed systems, especially for relation of the Huang-Rhys factors,

$$S_j^0 = \frac{1}{2\hbar}\omega_j^0 (d_j^0)^2 \rightarrow \frac{1}{2\hbar}\omega_j (d_j)^2 = S_j, \tag{7}$$

where (ω_j^0, d_j^0) and (ω_j, d_j) stand for unperturbed and perturbed normal-mode vibarational frequency and displacement, respectively.

Before applying damped harmonic oscillators method to simulate absorption and fluorescence spectra for perylene molecule, we introduce *ab initio* quantum chemistry methods employed for calculating the equilibrium geometries and vibrational frequencies of the ground state $S_0(^1A_g)$ and the first excited state $S_1(^1B_{1u})$ plus transition dipole oscillator strengths, vertical and adiabatic excitation energies. We have utilized the (time-dependent) density functional theory with functionals (TD)-B3LYP (i.e., B3LYP20), (TD)-B3LYP35, (TD)-B3LYP50 (i.e., BHandHLYP), and HF-CIS (i.e., B3LYP100). The numbers following after B3LYP stand for different hybrid exchange-correlation functionals containing 20% (B3LYP), 35%, 50%, and 100% (HF) of exact Hartree-Fock exchange of the density functional theory. The four basis sets, 6-31G(d), 6-31+G(d), 6-311G(d), and 6-311+G(d), have been tested as well. Although absolute equilibrium geometries of electronic states slightly depend on choice of basis sets, geometry differences between ground S_0 and excited S_1 states are almost independent on choice of basis sets (these differences determine the Huang-Rhys factors that are converted vibronic spectra from Eqs. (4) and (5)). The present calculations have been performed with PCM condition in benzene solvent and without PCM condition in gas phase. All calculations are carried out using GAUSSIAN 09 program package.[47]

III. APPLICATION TO ABSORPTION AND FLOURESCENCE SPECTRA OF PERYLENE

The electronic spectroscopy of polycyclic aromatic hydrocarbons is of particular interest since it provides a framework for the understanding of the electronic structure of large polyatomic molecules.[48–50] Polycyclic aromatic hydrocarbon molecules have received attention from fundamental studies towards a better understanding of molecular structure and dynamics, especially interaction with hydrogen atoms.[49] Polycyclic aromatic hydrocarbon molecules have high symmetry in which each hydrogen atom is approximately subjected to the same environment in solution, and thus scaling parameters to hydrogen atom can be approximately the same. This greatly simplifies empirical search of the scaling parameters. We take perylene molecule as a prototype of medium-sized polycyclic aromatic hydrocarbon, since its electronic spectra in both gaseous and solution phases have been extensively studied. However, the intensity enhancement of the vibronic spectra in solution has not been well understood theoretically as far as we know.

The lowest singlet excited state S_1 of perylene molecule has transition type of $\pi \rightarrow \pi^*$ through experimental absorption and fluorescence spectra both in gaseous phase[51–53] and in benzene solution.[45] Computational studies on equilibrium geometries and vibrational frequencies for ground- and the first-excited states of perylene and its electronic spectra have been performed.[44,54–56] Absorption and fluorescence spectra of perylene in gaseous phase were simulated with including both Duschinsky rotation and Herzberg–Teller effects,[44] it was found that the both effects are very small (one can compare Fig. 5(a) of Ref. 44 with Fig. 4 from the present simulation in gaseous phase). We think that the intensity enhancement of the vibronic spectra in solution might be attributed to the hydrogen atoms of perylene interacting with solvent molecules.

The present calculation confirmed that equilibrium geometries of perylene molecule in both ground and the first excited states have planar structure as D_{2h} point group

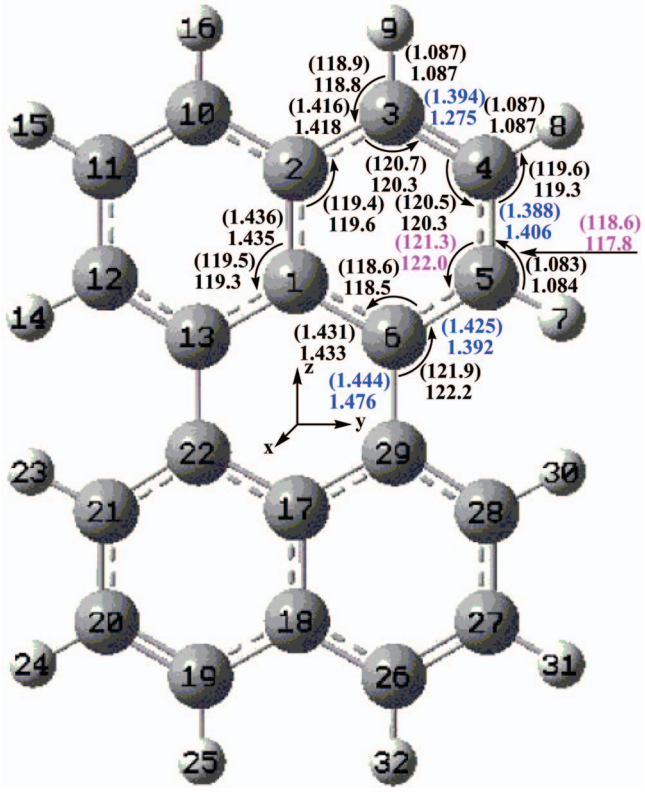

FIG. 1. Optimized geometries of the S_0 and S_1 states using B3LYP/6-31G(d) and TD-B3LYP/6-31G(d) without PCM condition. The bond lengths are in angstrom and angles in degree (parameters in the brackets for S_1, otherwise for S_0). Note that the optimized geometries of both S_0 and S_1 have D_{2h} group symmetry.

symmetry as shown in Fig. 1. This agrees well with the experimental results[51] and the previous calculation results.[44,51,56] Figure 1 shows the optimized geometries with (TD) B3LYP/6-31G(d) method in gas phase in which the bond lengths and angles in the S_0 and S_1 states are very similar. The bonds C3-C4 and C5-C6 are stretched by 0.02 Å and 0.03 Å, respectively, from S_0 to S_1 state; while the bond C4-C5 is shortened from 1.406 Å to 1.388 Å and the bond C6-C29 from 1.476 Å to 1.444 Å. It is also shown that the angle C4-C5-H7 is expanded by 0.8° and the angle C4-C5-C6 is reduced from 122.0° to 121.3° from S_0 to S_1 state. The other differences are 0.001–0.002 Å for bond lengths and 0.1°–0.5° for bond angles. On the other hand, the present calculation showed that the first excited state S_1 has a $\pi\pi^*$ transition feature, thus the significant changes in geometry comes from the CC bond lengths when $X\ ^1A_g \rightarrow A\ ^1B_{1u}$ transition occurs. Natural orbital analysis predicted that the S_1 state results mainly from the excitation of the HOMO → LUMO (one electron excited) as shown in Fig. 2. We have carried out calculation for equilibrium geometries of the S_0 and S_1 states with PCM in benzene solvent, and we found that the results are quite similar to those of without PCM condition.

By performing frequency calculations at equilibrium geometries of S_0 and S_1 states, we found 16 total symmetry a_g normal-mode frequencies out of 90 vibrational normal-mode frequencies and the present calculation agrees well with the experimental results.[51,57] The distributions of corresponding 16 Huang-Rhys factors are shown in Table I. We have carried out the frequency calculations with equilibrium geometries of S_0 and S_1 states calculated with PCM condition, and we found that the 16 Huang-Rhys factors are almost same as those calculated without PCM condition. Although TDDFT-PCM method does present changes of equilibrium geometries of ground and excited states individually, change of geometry difference between ground and excited states is small and thus it does not affect Huang–Rhys factors. However, adiabatic excitation energies corresponding to 0-0 vibronic transition are quite different, and (TD) B3LYP calculation estimated the adiabatic excitation energy as 2.74 eV (452 nm) without PCM and 2.63 eV (471 nm) with PCM in benzene. In addition, we checked with other two (TD) DFT hybrid functionals and CIS method; both (TD)B3LYP35

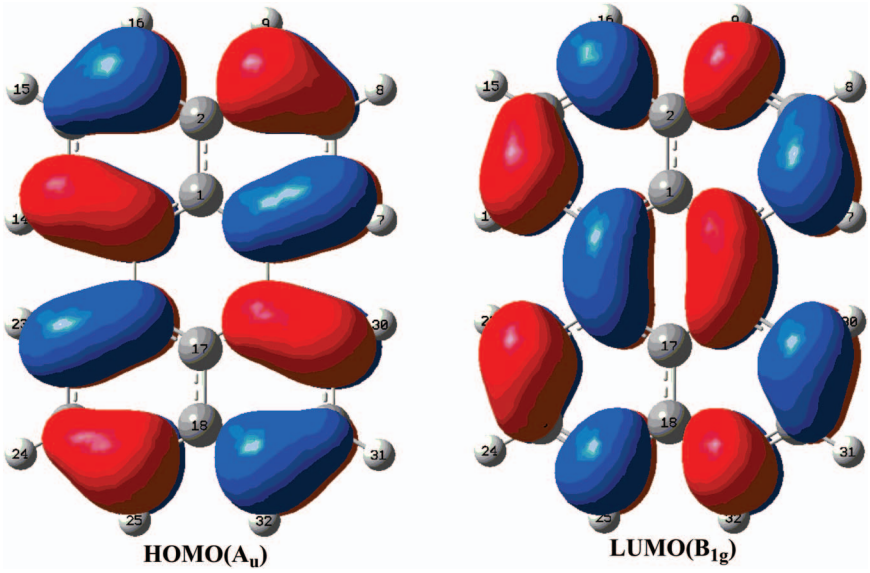

FIG. 2. Frontier molecular orbitals involved in S_0 (^1A_g) → S_1 ($^1B_{1u}$) excitation.

TABLE I. Experimental frequency (in cm $^{-1}$), and calculated vibrational normal-mode frequencies (ω_a, ω_b, ω_c, and ω_d) and Huang-Rhys factors (S_a, S_b, S_c, and S_d), corresponding to the scaling parameters chosen as ($\xi_H = 1.0$, $\xi_C = 1.0$), ($\xi_H = 1.2$, $\xi_C = 1.0$), ($\xi_H = 1.7$, $\xi_C = 1.0$), and ($\xi_H = 1.7$, $\xi_C = 1.2$), respectively, for ground state. The calculated frequency differences between S_0 (^1A_g) and S_1 ($^1B_{1u}$) states are shown as (s1-s0).

Total symmetry vibration modes (a_g)		Expt.[a](expt.[b])	$\xi_H = 1.0$, $\xi_C = 1.0$			$\xi_H = 1.2$, $\xi_C = 1.$		$\xi_H = 1.7$, $\xi_C = 1.$		$\xi_H = 1.7$, $\xi_C = 1.2$	
			ω_a	s1-s0	S_a	ω_b	S_b	ω_c	S_c	ω_d	S_d
1	Ring wagging	352(353)	358	− 1	0.250	356	0.254	349	0.241	324	0.260
2	Ring wagging	431(427)	436	0	0.006	431	0.008	418	0.016	404	0.021
3	Ring breathing	549(547)	556	− 2	0.098	552	0.11	541	0.113	506	0.115
4	Ring deform	803(801)	810	− 3	0.009	801	0.007	775	0.008	729	0.013
5	Ring deform		998	6	0.003	980	0.005	905	0.009	895	0.013
6	C-C stretch	–(1102)	1138	0	0.001	1089	0.002	965	0.002	944	0.001
7	C-C stretch + C-H bend		1225	4	0.004	1146	0.006	1031	0.004	1012	0.006
8		1307(1300)	1339	− 16	0.032	1276	0.011	1163	0.002	1136	0.000
9			1400	3	0.039	1368	0.022	1309	0.062	1260	0.038
10*		**1380(1372)**	**1410**	**10**	**0.077**	**1403**	**0.266**	**1398**	**0.359**	**1347**	**0.411**
11			1487	19	0.027	1452	0.03	1431	0.002	1390	0.003
12		1652(1580)	1619	− 35	0.075	1606	0.115	1590	0.182	1500	0.043
13		1660	1650	− 15	0.003	1633	0	1613	0.022	1552	0.161
14	C-H stretch	3072	3185	1	0.013	2941	0.019	2522	0.016	2493	0.013
15	C-H stretch		3203	0	0.021	2960	0.02	2543	0.035	2511	0.028
16	C-H stretch	3144	3232	11	0.054	2985	0.065	2562	0.047	2531	0.058

[a]From Ref. 51.
[b]From Ref. 57.

and (TD)B3LYP50 calculations have showed the same adiabatic excitation energy as 3.06 ev (405 nm) and 2.93 ev (423 nm), and CIS as 3.69 eV and 2.93 eV without PCM and with PCM in benzene solution, respectively, as shown in Table II. Adiabatic excitation energies with PCM are generally lower than those without PCM. This is also true for vertical excitation energies. The corresponding oscillator strengths are 0.36/0.49, 0.42/0.55, 0.46/0.60, and 0.70/0.85 without-PCM/with-PCM calculated by TD(B3LYP), TD(B3LYP35), TD(B3LYP50), and TD(B3LYP100), respectively. The more portion of Hartree-Fock exchange including in DFT hybrid exchange-correlation functionals, the stronger oscillator strengths are. Oscillator strengths are enhanced with PCM in benzene solution compared without PCM in gas phase. The present calculations for both vertical and adiabatic excitation energies show good agreement with experiment results[51,52] and comparison with the other theoretical simulations[44,58,59] is also shown in Table II.

TABLE II. Observed and calculated vertical and adiabatic excitation energies (E_{vert} (eV) and E_{ad} (eV)) with the calculated oscillator strengths (*f*) for $^1B_{1u}$ transition of perylene and discrepancies (Δ) of adiabatic excitation energy between theory and experiment.

	Vertical		Adiabatic	
	E_{vert} (eV)	*f*	E_{ad} (eV)	Δ (eV)
Expt.	2.96[a]		2.82[b]/2.98[c]	
TD (B3LYP)	2.9	0.3614	2.74	− 0.08/−0.24
TD (B3LYP)[d]	2.86	0.3616	2.7	− 0.12/−0.28
TD (BLYP)[a]	2.64	0.3088		
CIS	4.04	0.7015	3.69	0.87/0.71
TD (B3LYP)-PCM	2.8	0.4866	2.63	− 0.19/−0.35
TD (B3LYP35)	3.27	0.4201	3.06	0.24/0.08
TD (B3LYP35)-PCM	3.16	0.5510	2.93	0.11/−0.05
TD (BHandHLYP)	3.31	0.4565	3.06	0.24/0.08
TD (BHandHLYP)-PCM	3.2	0.6005	2.93	0.11/−0.05
CIS-PCM	3.9	0.8521	3.5	0.68/0.52

[a]From Ref. 52.
[b]From Refs. 58 and 59.
[c]From Ref. 51.
[d]From Ref. 44.

A. Vibronic spectra simulated in gaseous phase

Let us first simulate the absorption spectra of perylene in gaseous phase with setting homogeneous broadening as $\gamma_{ab} = 20\text{cm}^{-1}$ in Eq. (4) (reflecting the instrumental resolution broadening in experiment) and inhomogeneous broadening parameter D_{ab} as zero. Temperature is chosen as $T = 20$ K and the band origin (0-0 transition) is set up to be 23 883 cm^{-1} as it was adopted in experimental study.[52] Under displaced harmonic oscillator approximation, we found six modes with significant numbers of Huang-Rhys factors in the column ($\xi_H = 1.0$, $\xi_C = 1.0$) of Table I, their vibrational normal modes are shown in Fig. 3, and four of them that are most active for the main progressions of vibronic bands. The absorption spectrum are well described by ring wagging mode ν_1 (its Huang-Rhys factor $S_{\nu 1} = 0.250$) accompanied with ring breathing mode ν_3 ($S_{\nu 3} = 0.098$), C-H bend plus C-C stretch modes ν_{10} ($S_{\nu 10} = 0.077$) and ν_{12} ($S_{\nu 12} = 0.075$) calculated by (TD) B3LYP/6-31G(d). Huang-Rhys factors calculated from the other three (TD) DFT methods show the similar tendency as those calculated by (TD) B3LYP and they are not shown here. However, we do show simulated absorption spectra from HF-CIS, (TD) B3LYP, (TD) B3LYP35, and (TD) B3LYP50 methods, respectively, in Figures 4(b)–4(e). They all agree well with experimental observation as shown in

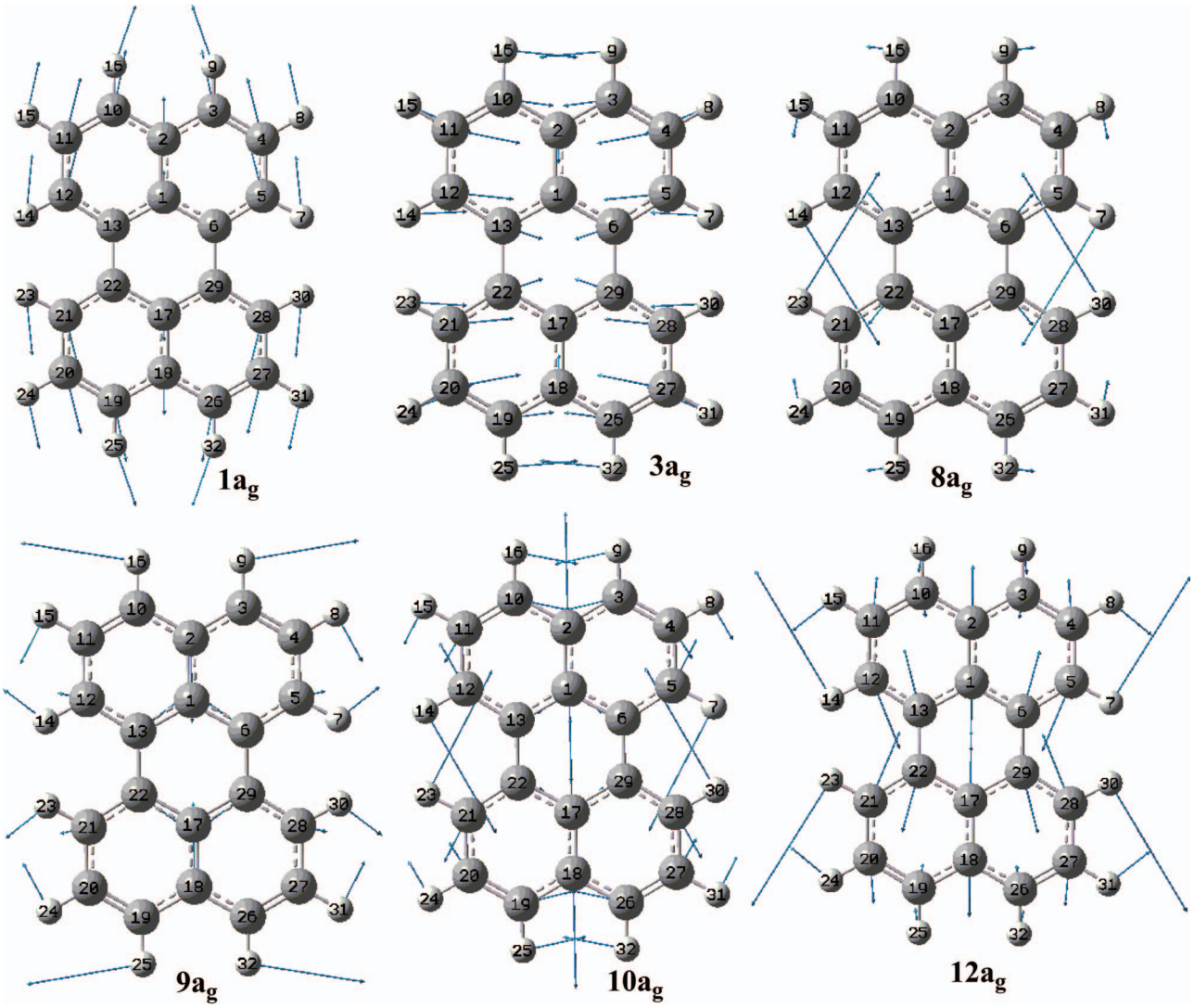

FIG. 3. Six active vibrational normal modes calculated at B3LYP/6-31G(d) level.

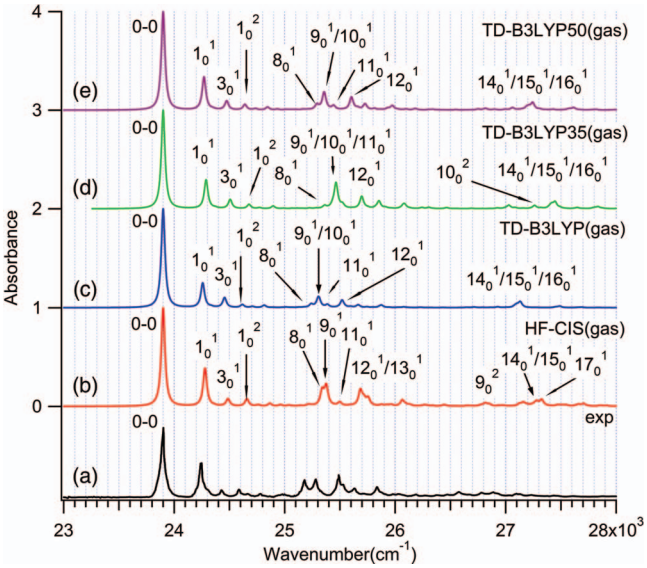

FIG. 4. S_0 (^1A_g) → S_1 ($^1B_{1u}$) absorption spectrum at temperature $T = 20$ K for perylene in gaseous phase without PCM condition. (a) Experimental data from Refs. 52 and 53, and simulations from (b) HF-CIS ((TD) B3LYP100), (c) (TD) B3LYP, (d) (TD) B3LYP35, and (e) (TD) B3LYP50.

Fig. 4(a). The main peak corresponding to 0-0 vibronic bands and the other vibronic bands are pretty weak. We have done simulation including the first-order anharmonic correction and its contribution is negligible. The Duschinsky and Herzberg–Teller effects were confirmed to be small for absorption spectra of $S_1(^1B_{1u})$.[44] We conclude that displaced harmonic oscillator is method good enough to reproduce experiment absorption spectra of perylene in gaseous phase. This makes perylene molecule as an ideal case to look for solvent enhanced vibronic spectra by damped harmonic oscillator method. This is our motivation of the present study, and in Subsection III C, we investigate robustness of the present method in terms of scaling parameters defined in Eqs. (2) and (3).

B. Vibronic spectra simulated with damped harmonic oscillator method in solution phase

By choosing inhomogeneous broadening parameters $D_{ab} = 300\,\mathrm{cm}^{-1}$ and $D_{ab} = 400\,\mathrm{cm}^{-1}$, respectively, for absorption and fluorescence spectra, we employ damped harmonic oscillator method to simulate vibronic spectra in benzene solvent

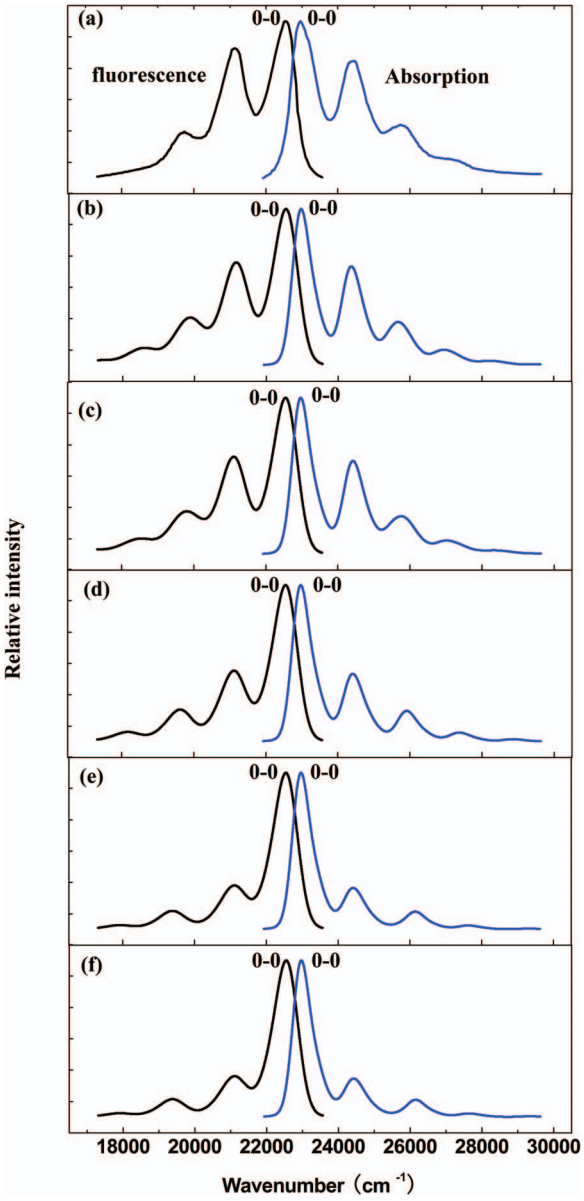

FIG. 5. Measured and calculated S_0 (^1A_g) → S_1 ($^1B_{1u}$) absorption and S_0 (^1A_g) ← S_1 ($^1B_{1u}$) fluorescence spectra at temperature T = 298 K for perylene in benzene solvent. (a) Experiment data from Ref. 45; simulated results with the scaling parameters: (b) $\xi_H = 1.7$, $\xi_C = 1.2$, (c) $\xi_H = 1.7$, $\xi_C = 1.0$, (d) $\xi_H = 1.2$, $\xi_C = 1.0$, (e) $\xi_H = 1.0$, $\xi_C = 1.0$ with PCM condition, and (f) $\xi_H = 1.0$, $\xi_C = 1.0$ without PCM condition.

environment. This is because that experiment measurement determines absorption and fluorescence width as 0.26 eV and 0.27 eV, respectively, at room temperature T = 298 K in benzene solvent,[50] and experiment observes spectrum shift (energy gap between the strongest peaks of absorption and fluorescence bands) as 422 cm^{-1}. With unscaled local force constants defined in Eq. (3) where all $\xi_i = 1$, the present simulation reproduces the strongest 0-0 vibronic bands and spectrum shift for both the absorption and fluorescence spectra as shown in Fig. 5(f) (without PCM environment) and Fig. 5(e) (with PCM environment). However, the second strongest bands enhanced in benzene solvent from experiment shown in Fig. 5(a) are not reproduced at all. The present simulation in gaseous phase did reproduce the weak band v_{10} of absorption as shown in Fig. 4.

We know that the reduced mass in Eq. (3) is close to hydrogen atom mass if diatom-like molecule contains hydrogen atom, and thus hydrogen atoms interacting with solvent molecules are most influential. By scaling every local mode related to hydrogen atom in perylene equally, we set up scaling parameters $\xi_i = \xi_H = 1.2$ and 1.7 with keeping all carbon atoms unscaled as $\xi_i = \xi_C = 1$. We obtained the corresponding Huang-Rhys factor of normal mode v_{10} shift to 0.266 (column with $\xi_H = 1.2$ in Table I) and 0.359 (column with $\xi_H = 1.7$ in Table I) from unscaled value 0.077. The other three active modes change slightly as shown in Table I. This shift of normal mode v_{10} is exactly responding to the second strongest band enhancement in benzene solvent, Figures 5(d) ($\xi_H = 1.2$ and $\xi_C = 1$) and 5(c) ($\xi_H = 1.7$ and $\xi_C = 1$) show the improving simulation of absorption and fluorescence spectra. If we further increases $\xi_H > 1.7$, the corresponding Huang-Rhys factor of normal mode v_{10} gradually decreases. Finally we have optimized scaling parameters $\xi_H = 1.7$ and $\xi_C = 1.2$, with which we have the Huang-Rhys factor of normal mode v_{10} shift to 0.411 (column with $\xi_C = 1.2$ in Table I. Then, we could reproduce the second and third strongest bands in benzene solvent as shown in Fig. 5(b). Especially, the simulated absorption and fluorescence spectral widths, 0.24 and 0.26 eV, respectively, are in very good agreement with the experimental values 0.26 eV and 0.27 eV. Figure 6 shows details of normal modes with $\xi_H = 1.7$ in comparison with $\xi_H = 1.0$ for enhanced absorption spectra, and it clearly shows that normal mode v_{10} to be most influential for the second and third strongest bands enhancement of absorption spectra in benzene solvent. It should be noted that there are four peaks in Fig. 6(a) while there are three peaks in Fig. 6(b). Scaling parameters with damped harmonic oscillator method could reproduce three peaks observed from experiment. We have checked various combinations of scaling ξ_H and ξ_C, and results showed very smooth and stable change with respect shift of the Huang-Rhys factors and normal mode frequencies within (TD) B3LYP method, and we should demonstrate more in Subsection III C.

C. Spectral robustness in terms of change of the scaling parameters

We have investigated how vibronic spectra of perylene vary with scaling parameters by employing (TD) B3LYP/6-31G(d) method. We found that Huang-Rhys factor of normal mode v_{10} increases as the scaling parameter ξ_H increases, while the other five active normal modes are almost unchanged. In order to fully understand and demonstrate that the present results are also valid as TFD functionals and basis sets change. In the present subsection, we employ (TD) B3LYP, (TD) B3LYP35, and (TD) B3LYP50 with basis set 6-311G(d) to check spectral robustness in terms of change of the scaling parameters. All simulations in the present subsection now are performed with perylene molecule in PCM benzene solvent environment, and the scaling parameters for all carbon atoms are fixed at $\xi_C = 1.0$, namely no scaling. The scaling parameters for all hydrogen atoms are considered at $\xi_H = 1.0$,

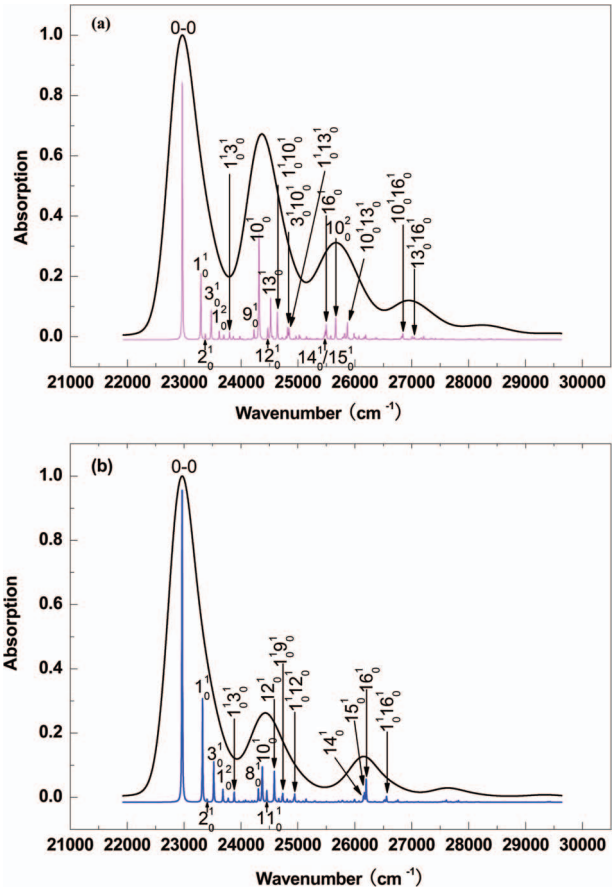

FIG. 6. Calculated S_0 (^1A_g) → S_1 ($^1B_{1u}$) absorption spectra at temperature T = 298 K for perylene in benzene solvent. Homogeneous and inhomogeneous broadening parameters are chosen as 20 cm^{-1} and 300 cm^{-1} for solvent (black line) and 5 cm^{-1} for assigned spectra (blue and pink line) in Franck-Condon simulation. Simulated results with the scaling parameter: (a) $\xi_H = 1.7$, $\xi_C = 1.2$ and (b) $\xi_H = 1.0$, $\xi_C = 1.0$ without PCM condition.

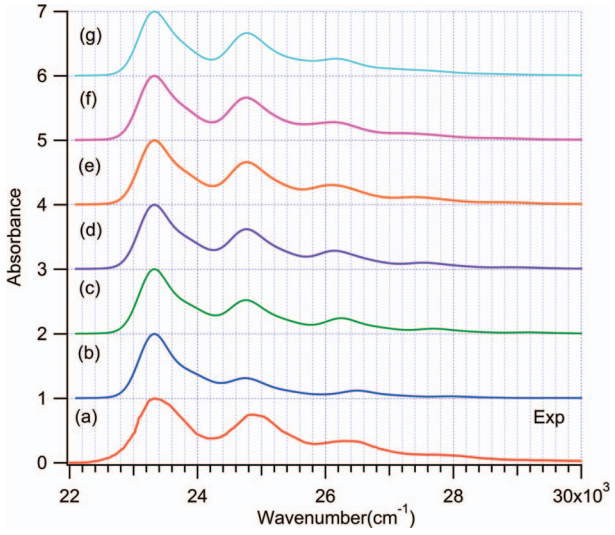

FIG. 7. Simulated absorption spectra from S_0 → S_1 for perylene by TD-B3LYP/6-311g(d) method with PCM in benzene solvent at temperature T = 298 K. Homogeneous and inhomogeneous broadening parameters are chosen to be 20 cm^{-1} and 300 cm^{-1}, respectively. (a) Experimental data from Ref. 45. Simulated data with scaling parameters $\xi_C = 1.0$ for all carbon atoms, but for all hydrogen atoms (b) $\xi_H = 1.0$, (c) $\xi_H = 1.2$, (d) $\xi_H = 1.4$, (e) $\xi_H = 1.6$, (f) $\xi_H = 1.8$, and (g) $\xi_H = 2.0$.

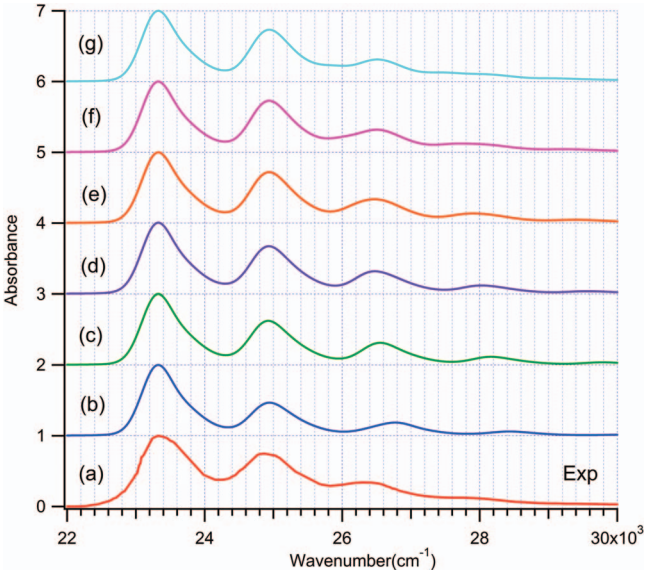

FIG. 8. The same as in Fig. 7 except simulation performed with TD-B3LYP35/6-311g(d) methods.

1,2, 1.4, 1.6, 1.8, and 2.0. Simulation confirms that Huang-Rhys factor of normal mode v_{10} increases as the scaling parameter ξ_H increases from all three functionals chosen above and Huang-Rhys factors for the other five active normal modes are almost unchanged. Detailed comparison about absorption spectra is shown in Fig. 7 simulated from TD (B3LYP) 6-311G(d), Fig. 8 from TD (B3LYP35) 6-311G(d), and Fig. 9 from TD (B3LYP50) 6-311G(d). All three functionals demonstrate that the intensity of the second strongest bands is enhanced as the rise of scaling parameter from 1 to 2. However, TD (B3LYP) and TD (B3LYP35) can keep change of the band shape in good agreement with experimental observation, while TD (B3LYP50) does not follow the experimental band shape nicely. Actually HF-CIS shows much worse

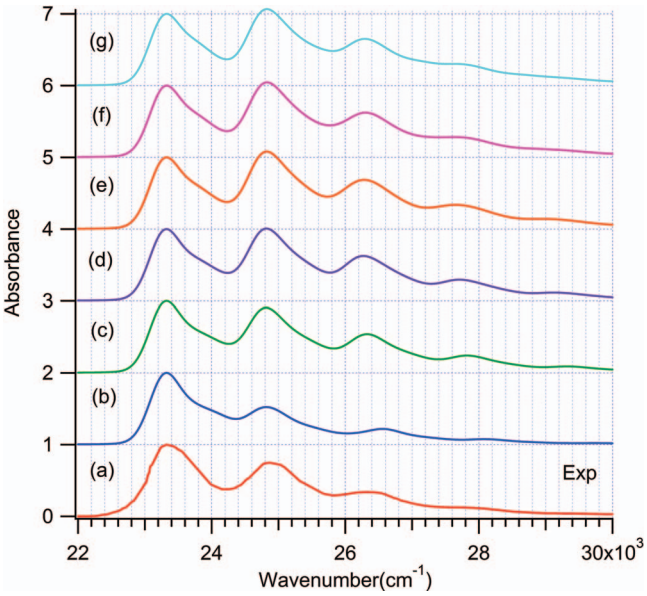

FIG. 9. The same as in Fig. 7 except simulation performed with TD-B3LYP50/6-311g(d) methods.

change of the band shape (not shown here). This means that the more exact Hartree-Fock exchange in hybrid exchange-correlation functionals is considered, the worse band shape is simulated. Something in between 20% and 35% for the exact Hartree-Fock exchange including in B3LYP functional performs the best simulation with the present damped harmonic oscillator method.

IV. CONCLUSION REMARKS

Staring with the displaced harmonic oscillator approximation to construct Franck-Condon factor, we have considered solute molecule vibrations in solution as damped harmonic oscillators and then we could obtain perturbed Franck-Condon factors from damping parameters related to local atom vibration in solute molecule. This is practically done by converting the mass-weighted molecular unperturbed Hessian matrix to perturbed Hessian matrix, and then by diagonalizing perturbed Hessian matrix, we obtain perturbed normal-mode frequencies and Huang–Rhys factor corresponding to solute molecule under damped solvent environment. Empirically searching scaling parameters are carried out by comparing simulated vibronic spectra with experimental observation in the present study. In this way, we add a new aspect of solvent effect for molecular spectra in solution besides the other effects like Duschinsky and Herzberg−Teller.

The present method is especially useful for polycyclic aromatic hydrocarbons in which hydrogen atom vibrations in solution can be considered almost equally, so that the same scaling factor is applied to all hydrogen atoms in polycyclic aromatic hydrocarbons. We have demonstrated that enhancement of absorption and fluorescence spectra of medium-sized polycyclic aromatic hydrocarbon, perylene molecule in benzene solution, and we found that vibrational normal mode v_{10} is most influential through local modes of solute hydrogen atoms interacting with solvent molecule. For highly symmetric molecules like perylene, local vibration modes between carbon and hydrogen atoms are all needed to be dealt with so that a single damping parameter work well to reproduce solvent enhanced spectra. For molecule with less symmetry and many different species of atoms, local vibration modes can be very different and then multiple scaling parameters have to be introduced to simulate spectra. Initially multiple scaling parameters might be selected by focusing on diatoms (local modes) in molecule, and the same diatoms have the same scaling parameters. After initial shooting of simulation of spectra, various optimized procedures for multiple scaling parameters can be applied to reproduce experimental spectra. Actually, we have found in the present study that spectra are not so sensitive scaling parameters and in the certain region, simulated spectra are all in good agreement with experiment.

Spectral robustness in terms of scaling parameters has been fully investigated by systematically performing simulation with (TD) B3LYP, (TD) B3LYP35, (TD) B3LYP50, and HF-CIS methods, and all methods demonstrate the same behavior of solvent enhanced absorption spectra against rise of scaling parameter for hydrogen atom in perylene. One of six active normal mode v_{10} is most responsible to solvent enhanced absorption spectra and this result is confirmed from all kind of (TD) B3LYP-like functionals. It should be emphasized that scaling parameters for C-H local modes mainly rotate normal modes slightly. However, in the present (displaced oscillator) calculations this rotation and (minor) change in frequencies is exactly the same in ground and excited states. The redefinition of normal modes changes the gradient of the excited state expressed in normal mode coordinates and this in turn scale Huang-Rhys factors to enhance the spectra in solution. The minor frequency shifts have little effect on enhancement of the spectra. We expect the principles of the phenomena: rotation of normal modes by change in mass/local mode factors to be similar even when Duschinsky rotation effects are included, but this is subject to further studies. We are now working on electronic spectra for large-sized polycyclic aromatic hydrocarbons in solution, and preliminary results show that the present method can reproduce vibronic spectra for large polycyclic aromatic hydrocarbons in solution even their vibronic spectra in gaseous phase are very different from those in solution phase. The present method can also follow spectral change for polycyclic aromatic hydrocarbons from one solvent to the other by adjusting scaling parameters. We will report those results in near future. In conclusion, we develop a practical method in calculating Franck-Condon factors perturbed by damped harmonic oscillator for vibronic spectra in solution.

ACKNOWLEDGMENTS

This work is supported by Ministry of Science and Technology of the Republic of China under Grant No. 100-2113-M-009-005-MY3. L.Y. thanks support from postdoctoral researcher of Aiming for the Top University Program under Grant No. 101W965 of the National Chiao-Tung University. C.Z. thanks the MOE-ATU project of the National Chiao Tung University for support.

[1]T. E. Sharp and H. M. Rosenstock, J. Chem. Phys. **41**, 3453 (1964).
[2]M. Roche, Chem. Phys. Lett. **168**, 556 (1990).
[3]E. V. Doktorov, I. A. Malkin, and V. I. Manko, J. Mol. Spectrosc. **64**, 302 (1977).
[4]S. Y. Lee, J. Phys. Chem. **94**, 4420 (1990).
[5]F. Zerbetto, J. Phys. Chem. **98**, 13157 (1994).
[6]P. T. Ruhoff, Chem. Phys. **186**, 355 (1994).
[7]P. A. Malmqvist and N. Forsberg, Chem. Phys. **228**, 227 (1998).
[8]T. Müller, P. H. Vaccaro, F. Perez-Bernal, and F. Iachello, J. Chem. Phys. **111**, 5038 (1999).
[9]D. K. W. Mok, E. P. F. Lee, F. T. Chau, D. C. Wang, and J. M. Dyke, J. Chem. Phys. **113**, 5791 (2000).
[10]H. Kikuchi, M. Kubo, N. Watanabe, and H. Suzuki, J. Chem. Phys. **119**, 729 (2003).
[11]H. Hwang and P. J. Rossky, J. Phys. Chem. A **108**, 2607 (2004).
[12]J. M. Luis, D. M. Bishop, and B. Kirtman, J. Chem. Phys. **120**, 813 (2004).
[13]A. Hazra, H. H. Chang, and M. Nooijen, J. Chem. Phys. **121**, 2125 (2004).
[14]M. Dierksen and S. Grimme, J. Chem. Phys. **122**, 244101 (2005).
[15]S. H. Lin, C. H. Chang, K. K. Liang, R. Chang, Y. J. Shiu, J. M. Zhang, T. S. Yang, M. Hayashi, and F. C. Hsu, Adv. Chem. Phys. **121**, 1 (2002).
[16]T. Petrenko, O. Krylova, F. Neese, and M. Sokolowski, New J. Phys. **11**, 015001 (2009).
[17]C. Zhu, K. K. Liang, M. Hayashi, and S. H. Lin, Chem. Phys. **358**, 137 (2009).
[18]B. Mennucci, C. Cappelli, C. A. Guido, R. Camlmi, and J. Tomasi, J. Phys. Chem. A **113**, 3009 (2009).
[19]J. Guthmuller and B. Champagne, J. Chem. Phys. **127**, 164507 (2007).
[20]G. Scalmani, M. J. Frisch, B. Mennucci, J. Tomasi, R. Cammi, and V. Barone, J. Chem. Phys. **124**, 094107 (2006).

[21]K. S. Schweizer and D. Chandler, J. Chem. Phys. **78**, 4118 (1983).
[22]L. A. Peteanua and D. H. Levy, J. Phys. Chem. **92**, 6554 (1988).
[23]J. Zeng, N. S. Hush, and J. R. Reimers, J. Chem. Phys. **99**, 1508 (1993).
[24]H. J. Kim, J. Chem. Phys. **105**, 6833 (1996).
[25]H. Nagae, J. Chem. Phys. **106**, 5159 (1997).
[26]I. Baraldi, G. Brancolini, F. Momicchioli, G. Ponterini, and D. Vanossi, Chem. Phys. **288**, 309 (2003).
[27]Y. H. Wang, M. Halik, C. K. Wang, S. R. Marder, and Y. Luo, J. Chem. Phys. **123**, 194311 (2005).
[28]H. C. Georg, K. Coutinho, and S. Canuto, J. Chem. Phys. **126**, 034507 (2007).
[29]O. V. Prezhdo, W. Boszczyk, V. V. Zubkova, and V. V. Prezhdo, J. Phys. Chem. A **112**, 13263 (2008).
[30]O. Clemens, M. Basters, M. Wild, S. Wilbrand, C. Reichert, M. Bauer, M. Springborg, and G. Jung, J. Mol. Struct.: THEOCHEM **866**, 15 (2008).
[31]D. C. Tranca and A. A. Neufeld, J. Chem. Phys. **130**, 141102 (2009).
[32]M. Dracinsky and P. Bour, J. Chem. Theory Comput. **6**, 288 (2010).
[33]I. F. Galvan, M. E. Martin, A. Munoz-Losa, M. L. Sanchez, and M. A. Aguilar, J. Chem. Theory Comput. **7**, 1850 (2011).
[34]T. Sakata, Y. Kawashima, and H. Nakano, J. Chem. Phys. **134**, 014501 (2011).
[35]W. Y. So, J. Hong, J. J. Kim, G. A. Sherwood, K. Chacon-Madrid, J. H. Werner, A. P. Shreve, and L. Peteanu, J. Phys. Chem. B **116**, 10504 (2012).
[36]Y. Shigemitsu, M. Uejima, T. Sato, K. Tanaka and Y. Tominaga, J. Phys. Chem. A **116**, 9100 (2012).
[37]J. E. Cotting, L. C. Hoskins, and M. E. Levan, J. Chem. Phys. **77**, 1081 (1982).
[38]T. Petrenko and F. Neese, J. Chem. Phys. **127**, 164319 (2007).
[39]F. J. A. Ferrer, V. Barone, C. Cappelli, and F. Santoro, J. Chem. Theory Comput. **9**, 3597 (2013).
[40]A. Baiardi, J. Bloino, and V. Barone, J. Chem. Theory Comput. **9**, 4097 (2013).
[41]F. Santoro, R. Improta, A. Lami, J. Bloino, and V. Barone, J. Chem. Phys. **126**, 084509 (2007).
[42]V. Barone, R. Improta, and N. Rega, Acc. Chem. Res. **41**, 605 (2008).
[43]T. W. Huang, L. Yang, C. Zhu, and S. H. Lin, Chem. Phys. Lett. **541**, 110 (2012).
[44]Q. Peng, Y. Niu, Z. Wang, Y. Jiang, Y. Li, Y. Liu, and Z. Shuai, J. Chem. Phys. **134**, 074510 (2011).
[45]S. J. Strickler and R. A. Berg, J. Chem. Phys. **37**, 814 (1962).
[46]H. C. Corben and P. Stehle, *Classical Mechanics*, 2nd ed. (Dover Publication, Inc., New York, 1994).
[47]M. J. Frisch, G. W. Trucks, H. B. Schlegel *et al.*, Gaussian 09, Revision C.01, Gaussian, Inc., Wallingford, CT, 2010.
[48]M. Hammonds, A. Pathak, and P. J. Sarre, Phys. Chem. Chem. Phys. **11**, 4458 (2009).
[49]J. A. Sebree, V. V. Kislov, A. M. Mebel, and T. S. Zwier, J. Phys. Chem. A **114**, 6255 (2010).
[50]J. A. Sebreez and T. S. Zwier, Phys. Chem. Chem. Phys. **14**, 173 (2012).
[51]Y. Kowaka, Y. Suganuma, N. Ashizawa, N. Nakayama, H. Goto, T. Ishimoto, U. Nagashima, and M. Baba, J. Mol. Spectrosc. **260**, 72 (2010).
[52]T. M. Halasinski, J. L. Weisman, R. Ruiterkamp, T. J. Lee, F. Salama, and M. Head-Gordon, J. Phys. Chem. A **107**, 3660 (2003).
[53]C. Joblin, F. Salama, and L. Allamandola, J. Chem. Phys. **110**, 7287 (1999).
[54]K. K. Ong, J. O. Jensen, and H. F. Hameka, J. Mol. Struct.: THEOCHEM **459**, 131 (1999).
[55]V. Baranov and A. Solov'yov, J. Struct. Chem. **40**, 199 (1999).
[56]X. F. Tan and F. Salama, J. Chem. Phys. **122**, 084318 (2005).
[57]B. Fourmann, C. Jouvet, A. Tramer, J. M. Lebars, and P. Millie, Chem. Phys. **92**, 25 (1985).
[58]K. H. Koch and K. Mullen, Chem. Ber. **124**, 2091 (1991).
[59]A. Bohnen, K. H. Koch, W. Luttke, and K. Mullen, Angew. Chem., Int. Ed. Engl. **29**, 525 (1990).